Numerical method for the nonlinear Fokker-Planck equation

D. S. Zhang, G. W. Wei, and D. J. Kouri
Department of Chemistry and Department of Physics, University of Houston, Houston, Texas 77204-5641

D. K. Hoffman
Department of Chemistry and Ames Laboratory, Iowa State University, Ames, Iowa 50011
(Received 24 January 1997)

A practical method based on distributed approximating functionals (DAFs) is proposed for numerically solving a general class of nonlinear time-dependent Fokker-Planck equations. The method relies on a numerical scheme that couples the usual path-integral concept to the DAF idea. The high accuracy and reliability of the method are illustrated by applying it to an exactly solvable nonlinear Fokker-Planck equation, and the method is compared with the accurate K-point Stirling interpolation formula finite-difference method. The approach is also used successfully to solve a nonlinear self-consistent dynamic mean-field problem for which both the cumulant expansion and scaling theory have been found by Drozdov and Morillo [Phys. Rev. E **54**, 931 (1996)] to be inadequate to describe the occurrence of a long-lived transient bimodality. The standard interpretation of the transient bimodality in terms of the ''flat'' region in the kinetic potential fails for the present case. An alternative analysis based on the effective potential of the Schrödinger-like Fokker-Planck equation is suggested. Our analysis of the transient bimodality is strongly supported by two examples that are numerically much more challenging than other examples that have been previously reported for this problem. [S1063-651X(97)07907-5]

PACS number(s): 02.70.Rw, 05.40.+j, 02.50.−r, 52.65.Ff

I. INTRODUCTION

Microscopic systems, whose dynamics are governed classically by the Liouville equation and quantally by the von Neumann equation, are time reversible. However, both equations are not soluble except under very special conditions. Reduced descriptions are standardly obtained using the Bogoliubov-Born-Green-Kirkwood-Yvon (BBGKY) hierarchy, Zwanzig's equation, or, equivalently, Mori's generalized Langevin equation, but these equations are still exact and thus, in general, also not soluble. However, appropriate truncation can lead to nonlinear equations describing macroscopic irreversible phenomena, such as the relaxation of thermodynamic systems that are far from equilibrium and the macroscopic self-organization of hierarchical biological systems. For a wide class of problems a useful but much simpler description is often given by the Fokker-Planck equation, which is a mesoscopic kinetic equation incorporating a deterministic drift vector and a chaotic diffusion tensor. The simplicity and the flexibility of the Fokker-Planck equation make it a popular kinetic equation both for theoreticians and for experimentalists. Theoretical aspects of the Fokker-Planck equation, stimulated by new experimental findings, are still under intensive studies. On the other hand, a variety of new experimental phenomena, some anticipated by theory, have been found to be well described by the Fokker-Planck equation. This synergism between experiment and theory, coupled with ever-increasing computer power, has spurred intensive efforts to obtain accurate numerical solutions of the Fokker-Planck equation efficiently. Analytical solutions, valuable in their own right as well as for testing new numerical methods, are available for only a few simple cases. For more complicated problems, both analytical and numerical methods are indispensable since the former yield a conceptual basis for understanding the physics described by the Fokker-Planck equation and the latter provide detailed solutions.

The numerical solution of the Fokker-Planck equation and in particular the nonlinear form of this equation, is still a challenging problem. Various approaches have been explored for obtaining numerical solutions. Suzuki's scaling theory [1] and normal mode analyses [2] have both proved useful for obtaining approximate solutions. However, scaling theory is accurate only to a few percent for intermediate times (i.e., those between the initial and equilibrium states) in the case of a linear bistable system [3] and normal mode analyses may suffer from slow convergence for general problems. A cumulant moment method has been used successfully by Desai and Zwanzig [4] for a nonlinear self-consistent dynamic mean-field model [5]. The slow convergence of the cumulant hierarchy was later observed in a study of a transient bimodality carried out by Brey, Casado, and Morillo [6]. Path-integral methods have been utilized by a number of authors [7–9]. Wehner and Wolfer [10] have presented a practical formalism that numerically evaluates the path integrals involving the Onsager-Machlup functionals and reduces the errors to a few percent. Monte Carlo techniques [11] are useful for providing information about certain properties of the system in terms of the moments of the stochastic process without the need for direct reference to the probability density distribution. In the case where the entire distribution function is required, direct approaches, such as those based on an eigenfunction expansion [12,13] or finite-difference methods [14–16], are frequently used. The eigenfunction expansion method is applicable to a general class of linear problems. Through this approach, various spectral methods can be used to provide extremely accurate solutions of the Fokker-Planck equation. In particu-

lar, by utilizing nonclassical weight functions that can be adapted to the problem under study, Shizgal's method [17] has been shown [3] to be superior to most others in terms of accuracy. The finite-difference method is known to lead often to stiff systems of ordinary differential equations with respect to the time. Chang and Cooper [18] have discussed a practical finite-difference procedure that allows the distribution function to evolve in a quasiequilibrium manner and preserves the number density of the system (in the absence of external sources or sinks). Larsen *et al.* [19] generalized the Chang-Cooper method to allow a large time increment and achieve greater numerical stability for a wide class of systems, including the nonlinear Compton problem. Their approach, however, depends on having analytic expressions for the collision parameters, which, in general, are not available for other applications. Recently, Epperlein [20] further generalized the Chang-Cooper method by taking into account energy conservation. His fully conservative scheme has been successfully applied to the Coulomb collision problem of a spatially homogeneous plasma. Drozdov and Morillo [21] have presented an elegant K-point Stirling interpolation formula finite-difference method, which provides a high level of accuracy without much increase in the number of spatial grid points required. Their method has been successfully applied to the nonlinear self-consistent dynamic mean-field Fokker-Planck equation [5].

The purpose of the present work is twofold. First, we utilize a distributed approximating functional [22,23] (DAF) based time-dependent method for the solution of the nonlinear Fokker-Planck equation. The reliability and accuracy of this DAF-based method are tested by considering an analytically solvable, nonlinear example problem. Second, we apply the method to a numerically more challenging problem: the nonlinear self-consistent dynamic mean-field model, introduced by Kometani and Shimizu [5] to describe the mutual controlling and regulating interaction between a macroscopic biological supersystem and its weakly (Weiss-field) coupled microscopic subsystems [4,24,25]. Desai and Zwanzig [4] reconsidered this model and derived the nonlinear self-consistent dynamic mean-field Fokker-Planck equation using both the cumulant method and a BBGKY hierarchical approach. An interesting, non-Gaussian equilibrium distribution and a nonlinear order-disorder phase transition were found by these authors using the former expansion method. Additional formal analyses were later given by Dawson [24]. The present choice of this numerical example is motivated by the numerical study given recently by Drozdov and Morillo [21]. They found an interesting, long-lived transient bimodality in a globally monostable case, which results in slow convergence of the cumulant hierarchy and the failure of Suzuki's scaling hypothesis. Another important aspect of their findings is that the standard kinetic potential method [26] fails to predict the occurrence of the long-lived bimodality. We are particularly interested in the causes of this failure and for this reason we analyze the validity of the conventional kinetic potential method. It is found that this method provides correct dynamical information if the generalized diffusion coefficient is of order unity. An alternative analysis for the transient bimodality based on the effective potential of the Schrödinger-like Fokker-Planck equation is proposed. The present analysis of the long-lived transient bimodality emphasizes the competition between the monostable oriented nonlinear effect and the random diffusion effect inside the effective potential. Our analysis is strongly supported by two special examples that we consider. One of these is characterized by an extremely long-lived transient bimodality and the other by a very short transient bimodality due to an extremely large relative nonlinear effect.

This paper is organized as follows. First, a review of the DAF formalism and a practical DAF-based space-time discretization scheme are presented in Sec. II. For the purpose of this presentation, we review only one particular DAF formalism, namely, the Hermite DAF, which we use throughout this work; however, we note that there is an ongoing effort devoted to the further theoretical development of DAFs. The DAF-based space-time discretization scheme is very simple and straightforward. It has some features similar in spirit to most finite-difference schemes. In this section a comparison to the formal derivation of the linear Fokker-Planck equation is also made. The reliability and accuracy of the present method is demonstrated using an exactly solvable Fokker-Planck equation. Section III is devoted to the numerical study of the nonlinear self-consistent dynamic mean-field Fokker-Planck equation. We first give a brief description of the equation and then compare our results with those of Drozdov and Morillo [21]. An explanation for the presence of a long-lived transient bimodality is presented. We end with a brief summary of our conclusions in Sec. IV

II. METHOD

This section consists of three subsections. The DAF formalism is reviewed in Sec. II A. In Sec. II B a DAF-based space-time discretization scheme is proposed. Finally, a numerical test of the present method is given in Sec. II C.

A. The distributed approximating functional formalism

Distributed approximating functionals have been introduced [22,23] as an *approximate* mapping of a certain set of continuous L^2 functions to itself, accurate to a given tolerance. This set of functions is termed the ''DAF class'' of functions. Again to a specified accuracy, the DAFs can be chosen so that the approximate mapping samples the class of functions of interest only on a discrete set of points. One of the important properties associated with the most commonly used *continuous* DAF mapping is that it is *always* well tempered, by which term we mean that both the DAF-class functions and their derivatives are approximated to the same level of approximation. (However, the approximation is not necessarily to the same level of accuracy since derivatives do not necessarily lie in the DAF class.) We remark that the DAF mapping is *exact* for polynomials of degree $M+1$, where M is the highest degree polynomial being used in constructing the DAF. Polynomials, of course, are *not* L^2 and this behavior is related to the fact that the DAFs yield an approximate, rather than exact, mapping on the Hilbert space of L^2 functions.

The ability of the DAF to provide an analytic representation of a function and its derivatives in terms of values of the function given only a discrete grid is central to its successful use in various computational applications. A variety of real-

izations of DAFs have been proposed, depending on the nature of the application of interest. We limit the following discussion to the Hermite DAF, which is the form utilized exclusively in the present work.

The Dirac δ function is defined to have the properties

$$f(x)=\int_{-\infty}^{\infty}\delta(x-x')f(x')dx', \tag{1}$$

$$f^{(l)}(x)=\int_{-\infty}^{\infty}\delta^{(l)}(x-x')f(x')dx'. \tag{2}$$

However, relations (1) and (2) are of little numerical utility for practical computations because they cannot be approximated directly by quadrature. In the DAF approach, an approximation to the $\delta(x-x')$ is constructed by using even Hermite polynomials H_{2n} [because $\delta(x)$ is symmetric in its argument] as

$$\delta_M(x-x'|\sigma)=\frac{1}{\sigma}\exp\left(\frac{-(x-x')^2}{2\sigma^2}\right)\times\sum_{n=0}^{M/2}\left(\frac{-1}{4}\right)^n\frac{1}{\sqrt{2\pi}n!}H_{2n}\left(\frac{x-x'}{\sqrt{2}\sigma}\right). \tag{3}$$

Obviously for *any* fixed σ, the Hermite DAF $\delta_M(x-x'|\sigma)$ becomes identical to the δ function when the maximal degree of the polynomial M goes to infinity, that is,

$$\lim_{M\to\infty}\delta_M(x-x'|\sigma)=\delta(x-x'). \tag{4}$$

Additionally, for fixed M, the Hermite DAF becomes identical to $\delta(x-x')$ in the limit $\sigma\to 0$, i.e.,

$$\lim_{\sigma\to 0}\delta_M(x-x'|\sigma)=\delta(x-x'). \tag{5}$$

In analogy to the functional properties given in Eqs. (1) and (2), the continuous DAF mappings are

$$f(x)\approx f_{\mathrm{DAF}}(x)=\int_{-\infty}^{\infty}\delta_M(x-x'|\sigma)f(x')dx', \tag{6}$$

$$f^{(l)}(x)\approx f^{(l)}_{\mathrm{DAF}}(x)=\int_{-\infty}^{\infty}\delta^{(l)}_M(x-x'|\sigma)f(x')dx', \tag{7}$$

where $\delta^{(l)}_M(x-x'|\sigma)$ is termed a ''differentiating DAF'' and is given by

$$\delta^{(l)}_M(x-x'|\sigma)=\frac{1}{2^{l/2}\sigma^{l+1}}\exp\left(\frac{-(x-x')^2}{2\sigma^2}\right)\sum_{n=0}^{M/2}\left(\frac{-1}{4}\right)^n\times(-1)^l\frac{1}{\sqrt{2\pi}n!}H_{2n+l}\left(\frac{x-x'}{\sqrt{2}\sigma}\right). \tag{8}$$

It is exactly the lth derivation of $\delta_M(x-x'|\sigma)$, in analogy to $\delta^{(l)}(x-x')$, occurring in Eq. (2). The Hermite DAF expressions, i.e., Eqs. (6) and (7), can be discretized by quadrature, thereby providing a computational scheme for generating *continuous* $f_{\mathrm{DAF}}(x)$ and $f^{(l)}_{\mathrm{DAF}}(x)$ from a knowledge of $f(x)$ on a discrete grid of points (the quadrature points). With an appropriate choice of M and σ, the Hermite DAF thus provides a controllable approximation to DAF-class functions at *any* x value of interest of the form

$$f(x)\approx f_{\mathrm{DAF}}(x)=\Delta\sum_i\ \delta_M(x-x_i|\sigma)f(x_i), \tag{9}$$

where Δ is the grid spacing. Moreover, the derivatives of the Hermite DAF provide a controllable approximation to $d^l[\,\delta(x-x')]/dx^l$ and therefore can be used to generate analytic approximations to derivatives for the DAF class of functions. Differentiating DAFs lead to an analytic representation of $f^{(l)}(x)$, at *any* point x in the domain of definition, according to

$$f^{(l)}(x)=\Delta\sum_i\ \delta^{(l)}_M(x-x_i|\sigma)f(x_i), \tag{10}$$

which is accurate if the derivatives are also in the DAF class. Equation (10), together with Eq. (8), implies that the differentiation operation has been converted into an algebraic operation in the DAF representation. This important feature makes the DAFs a powerful computational tool for solving various ordinary and partial differential equations. In particular, a given operator of the general form

$$L=A(x)+B(x)\frac{\partial}{\partial x}+C(x)\frac{\partial^2}{\partial x^2}+\cdots \tag{11}$$

has the Hermite DAF representation

$$L(x_i,x_j)=A(x_i)\delta_{ij}+B(x_i)\frac{\Delta}{\sqrt{2}\sigma^2}\exp\left(\frac{-(x_i-x_j)^2}{2\sigma^2}\right)\times\sum_{n=0}^{M/2}\left(\frac{-1}{4}\right)^n(-1)\frac{1}{\sqrt{2\pi}n!}H_{2n+1}\left(\frac{x_i-x_j}{\sqrt{2}\sigma}\right)+C(x_i)\frac{\Delta}{\sqrt{2}\sigma^3}\exp\left(\frac{-(x_i-x_j)^2}{2\sigma^2}\right)\times\sum_{n=0}^{M/2}\left(\frac{-1}{4}\right)^n\frac{1}{\sqrt{2\pi}n!}H_{2n+2}\left(\frac{x_i-x_j}{\sqrt{2}\sigma}\right)+\cdots. \tag{12}$$

This is the form that is most useful for ordinary differential equations and partial differential equations. It can also be used directly for numerical diagonalization in the case of an eigenvalue problem.

The most attractive properties of the Hermite DAF for solving differential equations can be summarized as follows. (i) It transforms ordinary and partial differentiations into operations with appropriate integral kernels, which when evaluated by quadrature involve their calculation to a matrix-vector multiplication. (ii) The global nature of spectral methods makes their practical application difficult for problems with complicated boundary conditions and complex geometry. By contrast, the Hermite DAF leads to highly banded matrix representations of derivatives, similar to finite-difference and finite-element methods. Thus the DAF

method possesses the best features of several earlier approaches. That is, the Hermite DAF has sufficient flexibility to handle complicated boundary conditions and geometries, like finite-difference and finite-element methods, but with an accuracy of the same order as spectral methods. In particular, since the DAF does not require a Gaussian or fixed sampling quadrature rule in its discretization, the number of grid points is not restricted by the degree of the polynomial. This implies that DAFs can be used for an arbitrarily large domain without increasing the size of the underlying polynomial set. (iii) Unlike spectral methods and finite-element methods, the DAF-based method is extremely simple and entails low CPU costs. The DAF matrix and its derivatives are calculated only *once* (in a computation requiring less than $\frac{1}{100}$ of a second in a typical calculation on an ordinary workstation) and once obtained can be used in a wide range of problems. In addition, $\delta_M^{(l)}(x-x')$ and $\delta_M(x-x')$ both depend only on $x-x'$ and, as a result, the DAF matrices (on an evenly spaced grid) have a Toeplitz structure. As a result, one needs to store only $W+1$ numbers for $\delta_M^{(l)}(x_i-x_j)$ (each l) and for $\delta_M(x_i-x_j)$ in order to generate all the various DAF matrices (here $2W+1$ is the DAF bandwidth). (iv) Furthermore, the DAF matrix acting on a vector can be evaluated by fast convolution, so the effort of evaluating expressions like Eqs. (9) and (10) scales as $N\log_2(2W+1)$, where N is the number of grid points. A numerical scheme based on this DAF formalism is outlined in the next subsection.

B. Numerical scheme

Consider a nonlinear Fokker-Planck equation of the general form

$$\frac{\partial f(x,t)}{\partial t}=\frac{\partial[A(x,f(x,t),t)f(x,t)]}{\partial x}+\frac{\partial^2[B(x,f(x,t),t)f(x,t)]}{\partial x^2}=L_{\mathrm{FP}}(f(x,t),t)f(x,t), \tag{13}$$

where the time dependence of the (pseudolinear) Fokker-Planck operator L_{FP} can arise from an implicit dependence on the distribution function $f(x,t)$ in the generalized drift coefficient $A(x,f(x,t),t)$ and the diffusion coefficient $B(x,f(x,t),t)$ and from an explicit dependence. From a numerical standpoint, it is helpful to symmetrize $L_{\mathrm{FP}}(f,t)f$ appropriately in order to take into account the dual roles of f since in the nonlinear case f appears both as a part of the operator and as the function on which the operator acts. This is illustrated, for a simple example of $L(f\,)f=f(\partial f/\partial x)$, by

$$L(f\,)=\frac{1}{2}\left[f\frac{\partial}{\partial x}+\frac{\partial f}{\partial x}\right]. \tag{14}$$

The symmetrized form of the Fokker-Planck operator $L_{\mathrm{FP}}(f\,)$ is assumed in the following discussion. In the case of forward time propagation we know both the function $f(x,t')$ and the operator L_{FP} at an earlier time t'. The function $f(x,t)$ at a later time t can be obtained by iterating Eq. (13),

$$\begin{aligned}f(x,t)&=\left[1+\int_{t'}^{t}dt_1L_{\mathrm{FP}}(f(x,t_1),t_1)+\int_{t'}^{t}dt_1\int_{t'}^{t_1}dt_2\right.\\&\left.\times L_{\mathrm{FP}}(f(x,t_1),t_1)L_{\mathrm{FP}}(f(x,t_2),t_2)+\cdots\right]f(x,t')\\&=\left[1+\sum_{n=1}^{\infty}\int_{t'}^{t}dt_1\int_{t'}^{t_1}dt_2\cdots\int_{t'}^{t_{n-1}}dt_n\right.\\&\left.\times L_{\mathrm{FP}}(f(x,t_1),t_1)\cdots L_{\mathrm{FP}}(f(x,t_n),t_n)\right]f(x,t').\end{aligned} \tag{15}$$

This form is *not* numerically practical since the matrices of the operators $L_{\mathrm{FP}}(f(x,t_n),t_n)$, and consequently the values of functions $f(x,t_n)$, are needed at all times t_n. In order to obtain a practical numerical form, we choose the time t_n such that $n(t_n-t_{n-1})=t-t'$ and use the Dyson time-ordering operator T. Thus Eq. (15) can be written as

$$\begin{aligned}f(x,t)&=T\left[1+\sum_{n=1}^{\infty}\frac{1}{n!}\int_{t'}^{t}dt_1\int_{t'}^{t}dt_2\cdots\int_{t'}^{t}dt_n\right.\\&\left.\times L_{\mathrm{FP}}(f(x,t_1),t_1)\cdots L_{\mathrm{FP}}(f(x,t_n),t_n)\right]f(x,t')\\&=T\exp\left[\int_{t'}^{t}ds\;L_{\mathrm{FP}}(f(x,s),s)\right]f(x,t').\end{aligned} \tag{16}$$

This is a convenient form for introducing approximations. For a sufficiently small time increment $\Delta t=t-t'$,

$$f(x,t)\approx\left[1+\sum_{n=1}^{R}\frac{1}{n!}[L_{\mathrm{FP}}(f(x,t'),t')\Delta t]^n\right]f(x,t'). \tag{17}$$

This expression should be useful so long as $f(x,t)$ does not vary rapidly with time or Δt is sufficiently small. It ignores errors associated with the commutator of L_{FP} at time t and $t+\Delta t$. We note that retaining more terms in the sum over n yields more accurate results, even though commutator terms in lower-order contributions have been neglected. Our expression (17) is different, which results from the stochastic derivation of a Fokker-Planck equation in which only the terms up to first order in Δt in the Kramers-Moyal expansion are kept. Numerical tests indicate that a truncation at the term that is linear in the operator L_{FP} ($R=1$, first-order approximation) is satisfactory for sufficiently small Δt. However, for a large Δt, it is necessary to retain the term that is quadratic in L_{FP} (i.e., $R=2$, or second order in L_{FP}) or terms of even higher order in L_{FP}, in order to achieve the desired accuracy and numerical stability.

For a given time t, the Hermite DAF representation of Eq. (17) is constructed according to Eq. (12). The robust nature of the DAF-based method is illustrated by applying it to two nonlinear Fokker-Planck equations, as discussed in the remainder of this paper. In the present computations, the Hermite DAF parameters are taken as $M=54$ and $\sigma=2.36\Delta$ for all cases.

C. Numerical test

In order to demonstrate the usefulness, test the accuracy, and explore the limitations of the DAF-based method for the nonlinear Fokker-Planck equation, we choose the following nonlinear model as a benchmark:

$$\frac{\partial f(x,t)}{\partial t}=\frac{\partial\{[\omega x+\theta\langle x(t)\rangle]f(x,t)\}}{\partial x}+D\,\frac{\partial^2 f(x,t)}{\partial x^2}, \tag{18}$$

where $\langle x(t)\rangle$ is the first moment of the distribution

$$\langle x(t)\rangle=\int_{-\infty}^{\infty}xf(x,t)dx \tag{19}$$

and ω, θ, and D are constant. Assuming an initial δ-function spatial distribution

$$f(x,0)=\delta(x-x_0), \tag{20}$$

the exact solution to Eq. (18) is

$$f(x,t)=\frac{1}{\sqrt{2\pi\sigma(t)}}\exp\left[-\frac{[x-\langle x(t)\rangle]^2}{2\sigma(t)}\right], \tag{21}$$

where $\langle x(t)\rangle$ and $\sigma(t)$ are given by

$$\langle x(t)\rangle=x_0e^{-(\omega+\theta)t} \tag{22}$$

and

$$\sigma(t)=\frac{D}{\omega}\,(1-e^{-2\omega t}), \tag{23}$$

respectively. By defining the second moment $M_2(t)$ as

$$M_2(t)=\langle x^2(t)\rangle-\langle x(t)\rangle^2, \tag{24}$$

the accuracy of the DAF-based method can be tested using a relative error defined by

$$\varepsilon(t)\equiv\frac{M_2(t)_R}{\sigma(t)}-1. \tag{25}$$

The subscript R indicates that the second moment $M_2(t)$ has been evaluated using the R-order approximate expansion (17) for the present numerical calculations. The relative error is plotted in Fig. 1 for $D=0.1$, $\omega=1$, $\theta=1$, and $x_0=1$. The time increment is taken as $\Delta t=0.01$ for all cases. Only 31 evenly spaced grid points, centered about the maximum of $f(x,t)$, are used for order $R=1$, 2, and 3, while slightly more grid points ($N=51$) are used for the fourth-order approximation ($R=4$) to demonstrate that the present method can easily achieve extremely high accuracy. The relative errors of the accurate results obtained by the K-point Stirling interpolation formula of Drozdov and Morillo [21] are also shown in the figure for comparison. Their results were also obtained using 31 grid points and a time increment of 0.01. They used an exponential power series expansion of the propagator to approximately determine $f(x,t)$ at small t's. Similarly, our computation starts from $t=0.1$ (In a more general case we just propagate the initial δ function.) It is seen that the higher the order of approximation, the better the results for the present time increment. In the case of small time increments, the effect of higher-order terms diminishes. For each given R, the present results are of the same or higher level of accuracy than those obtained by Drozdov and Morillo [21] using an appropriate K value. It should be noted that our R value does *not* correspond to their K value. The power of the present method is demonstrated by choosing $R=4$. In that case the relative error decreases to about 10^{-10}.

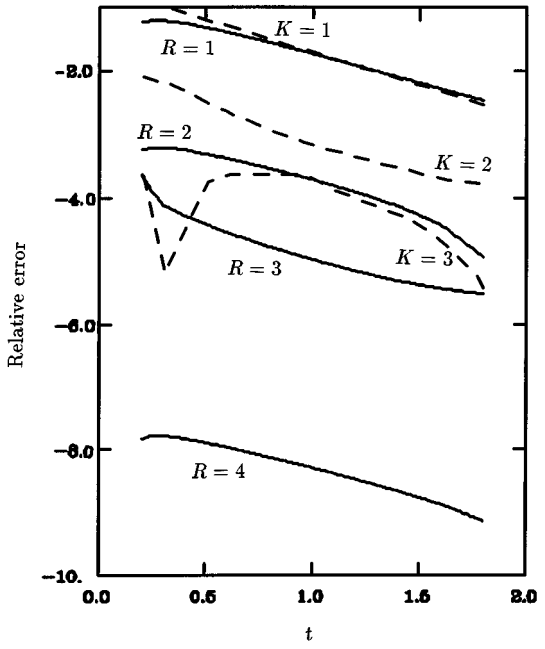

FIG. 1. Logarithm of the relative error $\log_{10}|\varepsilon(t)|$. Solid lines, present work; dashed lines, Ref. [21].

III. A NONLINEAR SELF-CONSISTENT DYNAMIC MEAN-FIELD FOKKER-PLANCK EQUATION

This section consists of two subsections. For charity of presentation, the nonlinear model is briefly reviewed in Sec. III A. The long-lived bimodal behavior, discovered by Drozdov and Morillo, is numerically confirmed in Sec. III B. A physical analysis of the phenomenon, based on the effective potential of the Schrödinger-like Fokker-Planck equation, is also given. The present interpretation is supported by two numerical examples, which are much more challenging than those reported previously.

A. Model

The nonlinear stochastic mean-field model was introduced by Kometani and Shimizu [5] as a physical model for muscle contraction. It describes the dynamics of a large number N of subsystems interacting through a mean field. In the large-N limit ($N\rightarrow\infty$) and using the molecular chaos assumption for the pair particle density operator, one obtains a true nonlinear Fokker-Planck equation [4] (13), namely,

$$\frac{\partial f(x,t)}{\partial t}=\frac{\partial\{[x^3+(\theta-1)x-\theta\langle x(t)\rangle]f(x,t)\}}{\partial x}+D\,\frac{\partial^2 f(x,t)}{\partial x^2}, \tag{26}$$

for the one-dimensional, ''one-particle'' distribution function $f(x,t)$ with a modified bistable drift force

$$A(x,t;f\ )=x^3+(\theta-1)x-\theta\langle x(t)\rangle \tag{27}$$

and Gaussian white noise

$$B(x,t;f\ )=D, \tag{28}$$

where $\langle x(t)\rangle$ is given by the instantaneous x mean

$$\langle x(t)\rangle=\int x\ f(x,t)dx. \tag{29}$$

This shows explicitly that the Fokker-Planck operator depends on the distribution function. Both θ and D are taken to be positive parameters. The equilibrium solution is of the non-Gaussian [4] form

$$f^{\rm eq}(x)=Z^{-1}\ \exp\left\{-\frac{1}{D}\left[\frac{x^4}{4}+(\theta-1)\ \frac{x^2}{2}-\theta\langle x\rangle_e x\right]\right\}, \tag{30}$$

where Z is the normalization factor and $\langle x\rangle_e$ is the equilibrium mean position

$$\langle x\rangle_e=\int x\ f^{\rm eq}(x)dx. \tag{31}$$

As discussed in great detail by Desai and Zwanzig [4], this system allows an ordered-disordered phase transition as one varies θ and/or D. The phase transition is characterized by a critical z_c line implicitly given by

$$\frac{\sqrt{2D_c}}{\theta_c}=\frac{\theta_c-1}{z_c\theta_c}=\frac{D_{-(3/2)}(z_c)}{D_{-(1/2)}(z_c)}, \tag{32}$$

where $D_{-n}(z)$ is a parabolic cylinder function. For given θ and D, z satisfies $z=(\theta-1)/\sqrt{2D}$ such that if $z<z_c$, the system is in the disordered phase with $\langle x\rangle_{e,0}=0$. If $z>z_c$, the system is in the ordered phase with three possible steady-state values of mean position: the metastable state $\langle x\rangle_{e,0}=0$ and globally stable states given by

$$\langle x\rangle_{e,\pm}=\pm\tfrac{1}{2}\{(2-\theta)+[(2+\theta)^2-24D]^{1/2}\}^{1/2}. \tag{33}$$

At the critical position $z=z_c$ the system will bifurcate between the two phases. It takes a long time for a given non-equilibrium state to attain equilibrium if the system is close to the critical line (the critical slowing down of the relaxation to equilibrium). Due to the nonlinearity, the system prefers only one steady state for the ordered phase, depending on the symmetry of the initial distribution $f(x,0)$. If the initial distribution $f(x,0)$ is symmetric with respect to $x=0$, then the system will be in the $\langle x\rangle_{e,0}=0$ steady state. If there is symmetry breaking (with respect to $x=0$) in the initial distribution $f(x,0)$, such as $\langle x(0)\rangle>0$ [or $\langle x(0)\rangle<0$], the nonlinearity will lead the system to a right ($\langle x\rangle_{e,+}$) chiral state [or a left ($\langle x\rangle_{e,-}$) chiral state]. We refer the reader to Desai and Zwanzig's excellent analysis [4] for more details.

B. Long-lived bimodality and interpretation

Numerical studies of this nonlinear Fokker-Planck equation have been conducted by a number of authors for a variety of states in the (θ,D) parameter space [4,6,21]. Desai and Zwanzig [4] studied five different states distributed in different regions of the phase diagram using both direct numerical simulations and the cumulant moment method. Their results indicate that the first few terms of the cumulant moment method provide both a qualitative physical picture of the problem and a very good approximation to the numerically exact results. Brey, Casado, and Morillo [6] later found that the cumulant moment method converges very slowly when the diffusion coefficient is small. They used Suzuki's scaling idea [1] to speed up their computation. A very recent numerical study by Drozdov and Morillo [21] shows an interesting long-lived transient bimodality before the chiral stable steady state is reached in the ordered phase. Their study indicates that both the cumulant moment method and the scaling theory break down when the long-lived bimodality occurs in this nonlinear case. It is well known that Suzuki's scaling theory provides a good approximation to the bistable dynamics in the linear case. What seems to make the discovery by Drozdov and Morillo most remarkable is, as argued by these authors, that there is no ''flat'' region in the kinetic potential $U(x,t)$,

$$U(x,t)=\frac{x^4}{4}+(\theta-1)\ \frac{x^2}{2}-\theta\langle x(t)\rangle x. \tag{34}$$

This is despite the fact that the flat region in the kinetic potential or the flat plateau in the corresponding force

$$F(x,t)=-\frac{\partial U(x,t)}{\partial x} \tag{35}$$

has been standardly associated with transient bimodality [26]. Thus Drozdov and Morillo's discovery presents an ob-

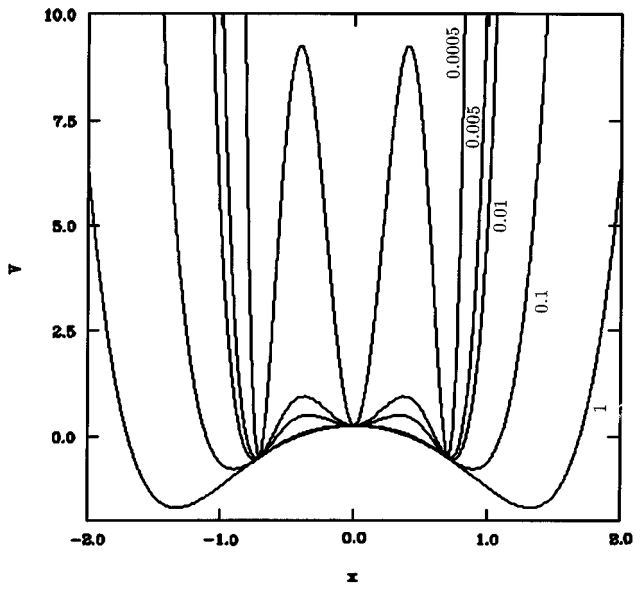

FIG. 2. Effective potential $V(x,t)$ of Eq. (36) for $\theta=0.5$, $t=0$, $\langle x(0)\rangle=0$, and $D=1.0$, 0.1, 0.01, 0.005, and 0.0005 from left to right (or from right to left).

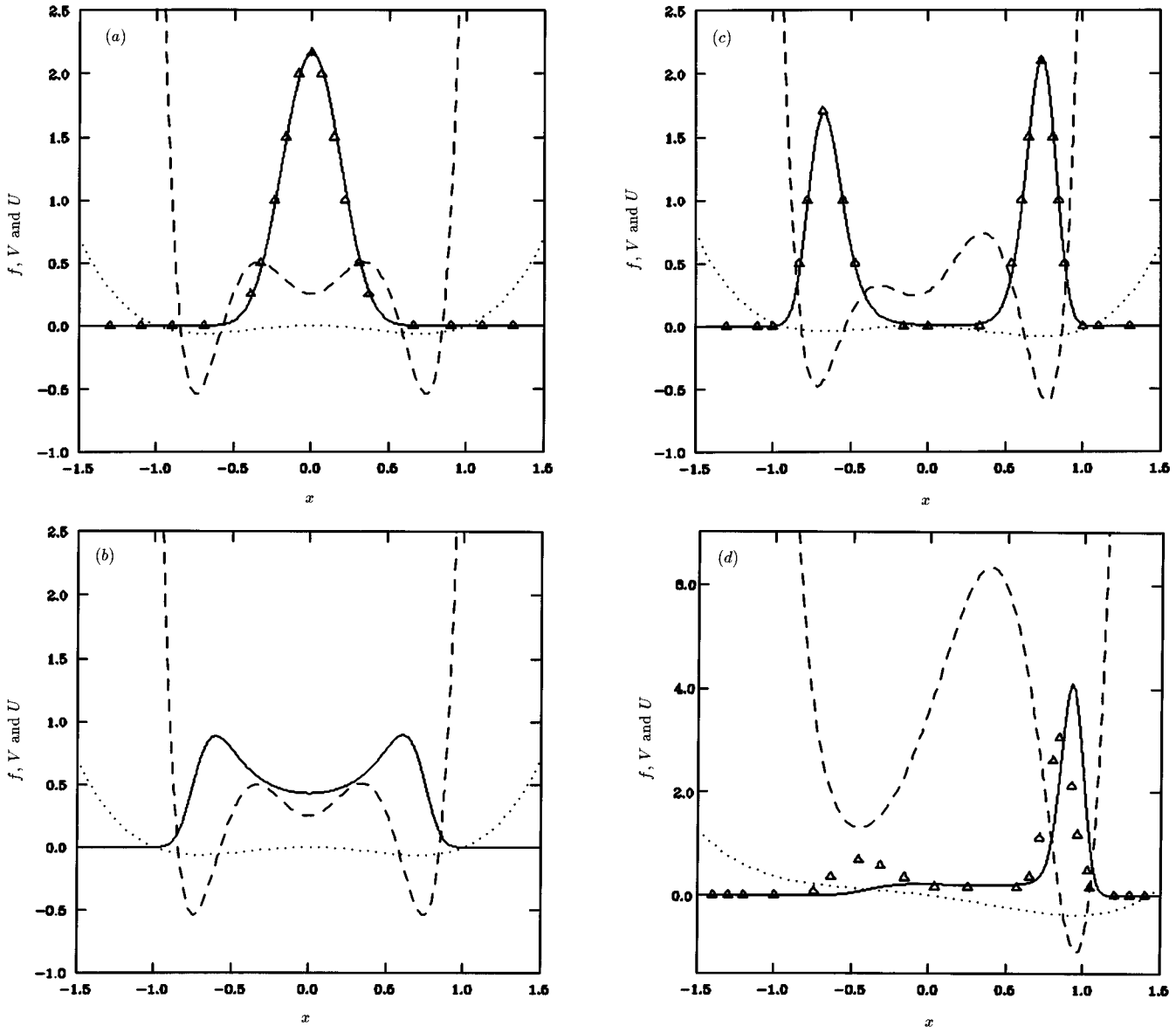

FIG. 3. Distribution function $f(x,t)$ (solid line), effective potential $V(x,t)$ of Eq. (36) (dashed line), and kinetic potential $U(x,t)$ of Eq. (34) (dotted line) for model (26) with $\theta=0.5$, $D=0.01$, and $\langle x(0)\rangle=10^{-4}$. (a) $t=1.0$, (b) $t=4.0$, (c) $t=72.0$, and (d) $t=105.5$. Triangles, $f(x,t)$ of Drozdov and Morillo [21].

stacle to the usual explanation of the occurrence of the long-lived transient bimodality. The purpose of the present study is to offer an alternative interpretation for the persistent transient phenomena. We note that the effective strength of the nonlinearity not only is determined by the size of θ, but also is influenced by the relative magnitude of the noise (the generalized diffusion coefficient). Therefore, it is not a surprise that the kinetic potential fails to describe the system qualitatively whenever the generalized diffusion coefficient is far from unity. We have found that the long-lived transient bimodality can be easily understood in terms of the effective potential $V(x,t)$,

$$V(x,t)=\frac{[x^3+(\theta-1)x-\theta\langle x(t)\rangle]^2}{4D}-\frac{1}{2}(3x^2+\theta-1), \tag{36}$$

which results from the transformation of the Fokker-Planck equation to a Schrödinger-like Fokker-Planck equation [27]. The corresponding Schrödinger-like Fokker-Planck equation for each given time t has the form

$$-D\frac{\partial^2\psi_n(x)}{\partial x^2}+V(x)\psi_n(x)=\varepsilon_n\psi_n(x), \tag{37}$$

where ε_n and $\psi_n(x)$ are the eigenvalue and eigenfunction, respectively. Here we refer the reader to Ref. [27] for more details about the transformation of the Fokker-Planck equation to the Schrödinger-like Fokker-Planck equation. It is noted that the effective potential $V(x,t)$ and the corresponding Schrödinger-like Fokker-Planck equation (37) are introduced for interpretational purposes. Computationally, we pursue Eq. (26) according to the method of Sec. II. Unlike the kinetic potential U, the effective potential V incorporates

the size of the diffusion coefficient to represent more closely the true size of the nonlinearity in the system. As a result, the occurrence of the bimodality is *entirely* predictable. For $\theta=0.5$, various $V(x,0)$ are plotted in Fig. 2 for several values of D. It is seen that $V(x,0)$ has a triple-well structure when D is very small. The smaller the D value, the deeper the central well. Obviously, the large humps near $x=0$ effectively block the initial wave packet (distribution function) from quickly escaping the metastable central well if it is placed there at $t=0$. However, this is not the sole effect because a small D means a large nonlinear effect. This causes the system to quickly reach the global stable equilibrium state. For a given θ, it is the combination of both the depth of the central well and the relative size of the nonlinearity that determines the occurrence of transient bimodality.

We first numerically confirm Drozdov and Morillo's findings by using the present DAF-based method. It is found that the $\langle x(t)\rangle$ and $M_2(t)$ obtained by the present approach for $\theta=2$, $D=0.1$, and $\langle x(0)\rangle=10^{-4}$ are in excellent agreement with the results of Drozdov and Morillo and with the sixth-order cumulant approximation for early times. At later times, the present results are closer to those of the cumulant method than to those of Drozdov and Morillo. We believe that our results are accurate for this regime. In this calculation, no significant transient bimodality is observed. However, for $\theta=0.5$, $D=0.01$, and $\langle x(0)\rangle=10^{-4}$, a long-lived transient bimodality appears from $t\approx4$ to 106. This is seen clearly from the distribution functions plotted in Fig. 3. Also plotted in Fig. 3 are the potentials $U(x,t)$ and $V(x,t)$. As pointed out by Drozdov and Morillo, $U(x,t)$ does not exhibit the flat region, which is standardly associated with the transient bimodality in bistable models [26]. The kinetic force $F(x,t)=-U'$, which has not been plotted, also does not show any flat plateau. Our analysis focuses on the effective potentials $V(x,t)$ of the Schrödinger-like Fokker-Planck equation. At initial times, $V(x,t)$ shows a typical triple-well structure. At earlier times the nonlinearity is very small [i.e., $\langle x(t)\rangle$ is small]. The dominant dynamical effect is the diffusion first inside the central well and later over two barriers. At $t=4$, most of the wave packet has moved outside the central well and reached two, almost equally deep, side wells. The nonlinearity eventually drives the wave packet to the right well, but it takes a long time for the wave packet to tunnel through the large central barrier. This explains the existence of persistent transient bimodality over the time period from $t=4$ to 105. The occurrence of the bimodality can also be seen from the $M_2(t)$ function, which, together with $\langle x(t)\rangle$, is plotted in Fig. 4. The failure of the cumulant expansion approximation [21] can be easily seen in this case. Our DAF results are in excellent agreement with those of Drozdov and Morillo at all times except for the period when the bimodality is disappearing. The Drozdov and Morillo's transient bimodality period is a bit longer than ours, which can also be seen from Fig. 3(d).

From the above analysis it is easy to predict that for given θ, decreasing D will lead to an even longer transient bimodality. This is indeed the case (for moderately small D values). As shown in Fig. 5, the transient bimodality period is more than 5910 time units for $\theta=0.5$, $D=0.005$, and $\langle x(0)\rangle=10^{-4}$. However, it is also true that decreasing the diffusion coefficient D leads to an effective increase in the relative nonlinearity. The nonlinearity becomes so important, even in the early times, that it dominates the dynamical process before the wave packet effectively diffuses over the two potential humps. This results in the disappearance of long-lived transient bimodality. As shown in Fig. 6, for $\theta=0.5$, $D=10^{-4}$, and $\langle x(0)\rangle=10^{-4}$, the monostable state is reached by $t=16$. Over the whole time period $M_2(t)$ is very small, which is the signature of small spreading of the wave packet. In fact, due to strong nonlinearity, the left peak exists for only a short time period and is very small during the course of the dynamical process. This is confirmed by the plot of the distribution function in Fig. 7. It is interesting to note that the usual-three-time-period pattern [4] for $M_2(t)$ does not appear in our case.

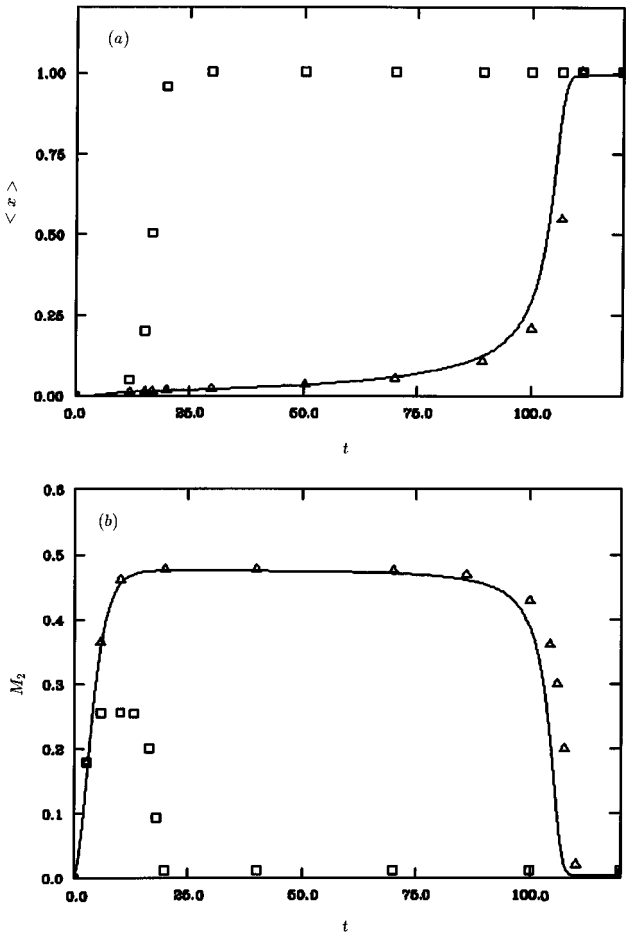

FIG. 4. Model (26) with $\theta=0.5$, $D=0.01$, and $\langle x(0)\rangle=10^{-4}$. (a) Plot of $\langle x(t)\rangle$ and (b) plot of $M_2(t)$. Solid lines, present results; squares, results of sixth-order cumulant approximation; triangles, results of Drozdov and Morillo [21].

We should point out that the two examples we consider are for values of the parameters that result in much more challenging computational problems than were considered earlier [4,6,21]. This provides strong support for the usefulness and reliability of the DAF-based method. It is believed that these two computational examples should also be valuable for providing a severe test for any prospective numerical methods for the field.

IV. CONCLUSION

In this paper a DAF-based method has been applied to the nonlinear Fokker-Planck equation. A practical numerical

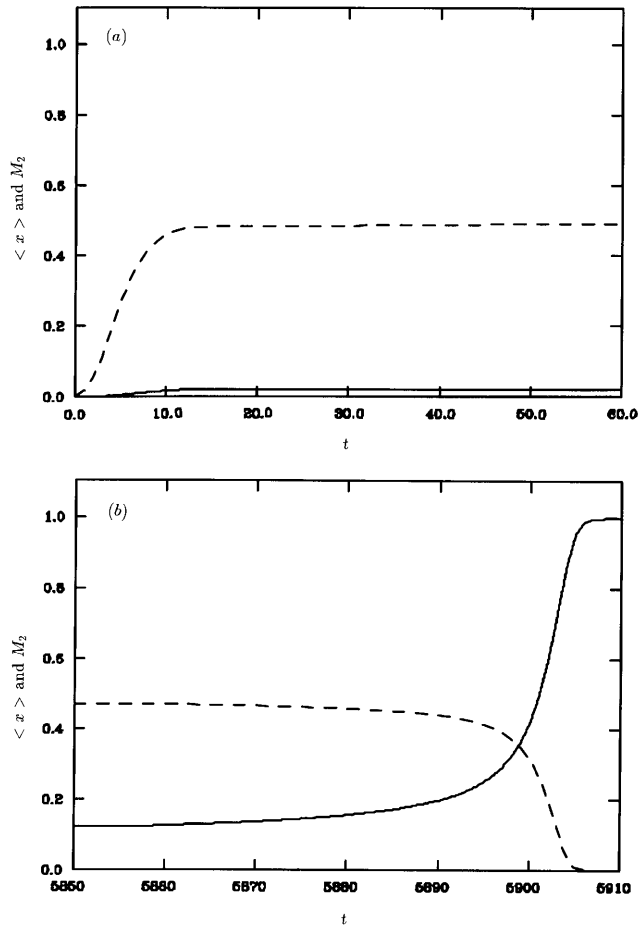

FIG. 5. Plot of $\langle x(t)\rangle$ (solid line) and $M_2(t)$ (dashed line) of model (26) with $\theta=0.5$, $D=0.005$, and $\langle x(0)\rangle=10^{-4}$.

scheme, which combines the usual path-integral concept (but which is *not* a path-integral method) with the DAF idea, is proposed and illustrated by example computations. The extension of the present method to two- and three-dimensional problems is straightforward and is under current consideration. The accuracy and reliability of our method has been demonstrated by application to an exactly solvable, nonlinear Fokker-Planck equation and compared with the accurate

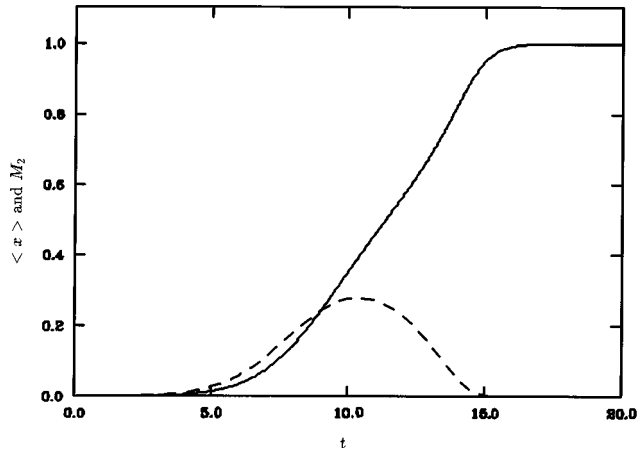

FIG. 6. Plot of $\langle x(t)\rangle$ (solid line) and $M_2(t)$ (dashed line) of model (26) with $\theta=0.5$, $D=10^{-4}$, and $\langle x(0)\rangle=10^{-4}$.

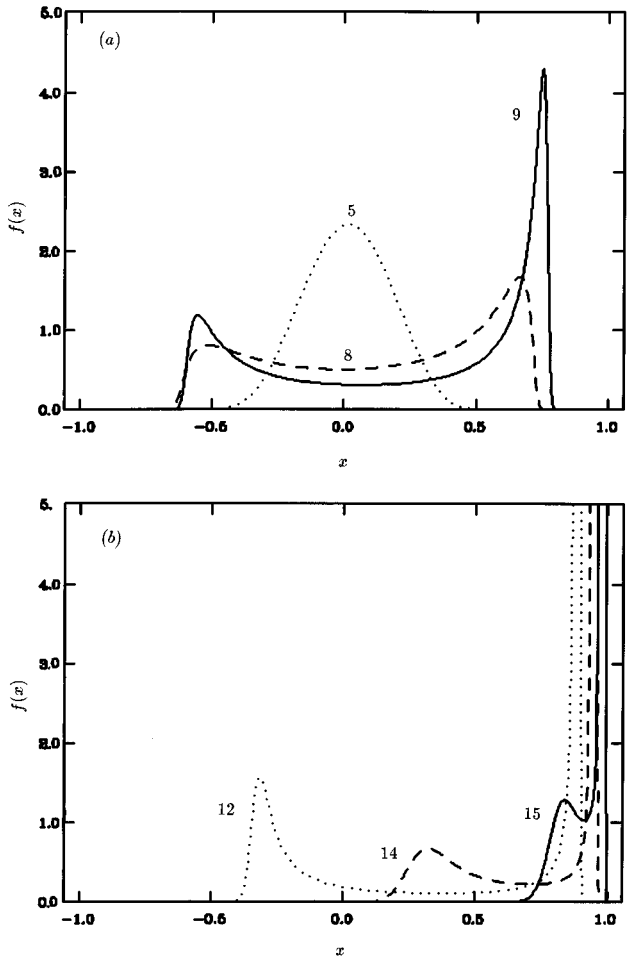

FIG. 7. Distribution function $f(x,t)$ for model (26) with $\theta=0.5$, $D=10^{-4}$, and $\langle x(0)\rangle=10^{-4}$ at $t=5$, 8, 9, 12, 14, and 15.

K-point Stirling interpolation formula finite-difference method [21]. It is found that the DAF-based method, while simple in its implementation, usually provides better, but always at least the same, level accuracy as the K-point Stirling interpolation formula. The power of the present method is demonstrated by the achievement of a relative precision of about 10^{-10} using only 51 grid points and a time increment of 0.01. It is easy for the present method to achieve even better precision, if that is needed for a problem under study, by either a slight increase in the number of grid points or a slight decrease in the time increment. A further, and much more challenging, test of the present method is the nonlinear self-consistent dynamic mean-field Fokker-Planck equation that allows an ordered-disordered phase transition. For $\theta=0.5$, $D=0.01$, two important approximation methods, namely, the cumulant expansion and Suzuki's scaling theory, have been previously shown [21] to fail to describe the occurrence of a long-lived transient bimodality. Here the present DAF-based method is shown to work very well for this case. Our DAF results are in excellent agreement with those of Drozdov and Morillo over all times except for the period when transient bimodality is disappearing. The present method is capable of solving two additional examples that are difficult to compute. One example ($\theta=0.5$, $D=0.005$) has a transient bimodality lasting more than 5910 time units. The other ($\theta=0.5$, $D=10^{-4}$) has a very strong

nonlinearity. These two examples provide a severe test of any computational method. It is believed that the present DAF based method will provide a rigorous numerical approach for handling a variety of statistical mechanical problems occurring in physics, chemistry, and biology.

Another important feature of the present study is the treatment of the nonlinear self-consistent dynamic mean-field Fokker-Planck equation [4], derived for a nonlinear muscle contraction model by Kometani and Shimizu [5]. The equilibrium properties and typical dynamical behavior of the problem have been excellently analyzed by Desai and Zwanzig [4]. A recent interesting development of the problem is due to Drozdov and Morillo [21]. They have found a long-lived transient bimodality for which both the cumulant expansion and Suzuki's scaling theory do not work. In addition to this, the long-lived transient bimodality turns out also to be a problem for the usual interpretation of the phenomenon in terms of a flat region of the kinetic potential $U(x,t)$ or its associated force $F(x,t)$. We note that for given θ and initial distribution, the appearance and disappearance of the long-lived transient bimodality are determined by the diffusion coefficient D, which is, however, *not* incorporated in the kinetic potential. This explains the failure of the standard interpretation. The present analysis employs the effective potential $V(x,t)$ of the Schrödinger-like Fokker-Planck equation, which can incorporate the generalized diffusion coefficient $B(x,t)$ (not just a constant D as in the present case). The effective potential $V(x,t)$ has a triple-well structure for small $\langle x(t)\rangle$ values and changes into a double-well structure as $|\langle x(t)\rangle|$ increases. It is important to note that the relative strength of the nonlinearity is also affected by size of D. For a given general nonlinear Fokker-Planck equation, we believe that the usual kinetic potential analysis works only if the generalized diffusion coefficient $B(x,t)$ is of order unity. The real dynamics is determined by the competition between the nonlinear motion, which tends toward to a global monostable value of $\langle x\rangle_e$, and the random diffusion process within the time-dependent effective potential $V(x,t)$. By using the present effective-potential-based analysis, we are able to explain qualitatively the occurrence and duration of the transient bimodality. Our analysis is strongly supported by two numerical examples. One of them, characterized by a small D, allows an extremely long transient bimodality. The other one, with an even smaller D, shows a very short transient bimodality due to the increase in the relative strength of the nonlinearity. It is hoped that the present effective-potential-based interpretation will be useful for the understanding of the dynamics of other nonlinear Fokker-Planck equations. In future work we plan to examine the application of the DAF-based method to the Fokker-Planck equation resulting from the standard eigenfunction expansion and compare it with Shizgal's method [3]. We also shall study two- and higher-dimensional linear and nonlinear Fokker-Planck equations.

ACKNOWLEDGMENTS

D.S.Z. was supported under R. A. Welch Foundation Grant No. E-0608. G.W.W. was supported under R. A. Welch Foundation Grant No. E-0608 and by NSERC. D.J.K was supported in part under National Science Foundation Grant No. CHE-9403416 and R. A. Welch Foundation Grant No. E-0608. The Ames Laboratory is operated for the Department of Energy by Iowa State University under Contract No. 2-7405-ENG82.

[1] M. Suzuki, Adv. Chem. Phys. **46**, 195 (1981).
[2] B. Caroli, C. Caroli, and B. Roulet, J. Stat. Phys. **26**, 83 (1981).
[3] R. Blackmore and B. Shizgal, Phys. Rev. A **31**, 1855 (1985).
[4] R. C. Desai and R. Zwanzig, J. Stat. Phys. **19**, 1 (1978).
[5] K. Kometani and H. Shimizu, J. Stat. Phys. **13**, 473 (1975).
[6] J. J. Brey, J. M. Casado, and M. Morillo, Physica A **128**, 497 (1984).
[7] H. Haken, Rev. Mod. Phys. **47**, 175 (1975).
[8] H. Grabert and M. S. Green, Phys. Rev. A **19**, 1747 (1979).
[9] H. Dekker, Phys. Rev. A **19**, 2102 (1979).
[10] M. F. Wehner and W. G. Wolfer, Phys. Rev. A **27**, 2663 (1983).
[11] D. L. Ermak and H. Buckholtz, J. Comput. Phys. **35**, 169 (1980).
[12] N. G. van Kampen, J. Stat. Phys. **17**, 71 (1977); H. Dekker and N. G. van Kampen, Phys. Lett. **73A**, 374 (1979).
[13] H. Tomita, A. Ito, and H. Kidachi, Prog. Theor. Phys. **56**, 786 (1976).
[14] P. D. Lax, Commun. Pure Appl. Math. **6**, 231 (1953).
[15] G. E. Forsythe and W. R. Wasow, *Finite Difference Methods for Partial Differential Equations* (Wiley, New York, 1967).
[16] V. Palleschi, F. Sarri, G. Marcozzi, and M. R. Torquati, Phys. Lett. A **146**, 378 (1990).
[17] B. Shizgal, J. Comput. Phys. **41**, 309 (1981).
[18] J. S. Chang and G. Cooper, J. Comput. Phys. **6**, 1 (1970).
[19] E. W. Larson, C. D. Levermore, G. C. Pomraning, and J. G. Sanderson, J. Comput. Phys. **61**, 359 (1985).
[20] E. M. Epperlein, J. Comput. Phys. **112**, 291 (1994).
[21] A. N. Drozdov and M. Morillo, Phys. Rev. E **54**, 931 (1996).
[22] D. K. Hoffman, N. Nayar, O. A. Sharafeddin, and D. J. Kouri, J. Phys. Chem. **95**, 8299 (1991).
[23] D. K. Hoffman and D. J. Kouri, J. Phys. Chem. **96**, 1179 (1992).
[24] D. Dawson, J. Stat. Phys. **31**, 29 (1983).
[25] M. Shiino, Phys. Rev. A **36**, 2393 (1987).
[26] M. Frankowicz, M. M. Mansour, and G. Nicolis, Physica A **125**, 237 (1984).
[27] H. Risken, *The Fokker-Planck Equation: Methods of Solution and Application* (Springer-Verlag, Berlin, 1984).